THESIS

NEURAL CORRELATES OF EXECUTED AND IMAGINED JOYSTICK DIRECTIONAL MOVEMENTS: A FUNCTIONAL NEAR-INFRARED SPECTROSCOPY STUDY

Submitted by

Matthew A. Mathison

Department of Psychology

In partial fulfillment of the requirements

For the Degree of Master of Science

Colorado State University

Fort Collins, Colorado

Fall 2019

Master's Committee:

Advisor: Donald C. Rojas

Deana Davalos
Chuck Anderson

ABSTRACT

NEURAL CORRELATES OF EXECUTED AND IMAGINED JOYSTICK DIRECTIONAL MOVEMENTS: A FUNCTIONAL NEAR-INFRARED SPECTROSCOPY STUDY

Motor-based brain computer interfaces (BCIs) attempt to restore and/or enhance motor functioning by measuring brain signals and converting them to computerized output. Functional near-infrared spectroscopy (fNIRS) is a non-invasive brain imaging modality that is resistant to both noise and motion-related artifacts. For this reason, fNIRS offers potential as an imaging method for use in a BCI. Currently, there is a paucity of literature on fNIRS as a sole BCI imaging method. Of the extant literature, studies were limited by low-density optode layouts and/or task designs which did not represent the motor goal. The present study was designed to enhance our understanding of the capabilities of fNIRS by utilizing a high-density optode array and an experimental task that closely mirrored the motor goal. 28 participants completed a series of executed and imagined joystick movements in four directions (forward, back, right, and left). Results indicated significant differences in inferred cortical activation during executed movements compared to baseline, executed movements compared to imagined movements, and imagined movements compared to baseline. No significant differences were observed for comparisons between individual movement directions. Results support the possibility that fNIRS may not be capable of distinguishing between changes in brain activity associated with joystick movement directions. Future research could enhance classification accuracy by implementing a machine learning algorithm or by pairing fNIRS with electroencephalography.

ACKNOWLEDGEMENTS

This project would not have been possible without the incredible people that have supported me throughout the years. I would like to express my sincere appreciation to committee members Dr. Deana Davalos and Dr. Chuck Anderson for their insightful feedback and encouragement during this project. I would also like to thank Dr. Don Rojas for his consistent support, excellent advise, and for the incredible amount of time invested in assisting me through the many challenges this project presented. I am sincerely grateful for all the help, support, and understanding I received from my family and friends. In particular, I offer my deep gratitude to my wife, A'Lece for standing by my side throughout this project, for lending an ear and/or proof-reading eye whenever needed, and for encouraging and motivating me from start to finish.

TABLE OF CONTENTS

INTRODUCTION

Brain computer interfaces have been developed primarily as a means to enhance or restore function to individuals with cortical damage or impairments. In 2013, 5.4 million Americans were reported to suffer from paralysis, 27% of which was caused by spinal cord injury (Armour et al., 2016). At present, the treatment outcomes for patients with permanent paralysis are highly limited, mostly focused on mobility aid and assistive technology. A brain computer interface (BCI) has the potential to enable individuals to interact with their environment without requiring the use of peripheral motor function. There are numerous forms of BCI taking a variety of approaches to restoring functions ranging from communication and wheelchair control to full command over advanced neuroprosthetics.

When developing a BCI, the primary challenge is acquiring and classifying brain signals. Currently, the most advanced systems used to measure brain signals involve surgical implantation of hardware onto the surface of the brain. While these methods have led to highly advanced BCIs (Velliste, Perel, Spalding, Whitford, and Schwartz, 2008; Collinger et al., 2013), they generate a significant amount of risk for the participant, including issues with tissue acceptance, risk of infection, and damage to cortical tissue with continued use over time (Nicolas-Alonso & Gomez-Gil, 2012).

Due to the risks and complications associated with invasive approaches to BCI, research has favored non-invasive neuroimaging methods. Due to its high temporal resolution, electroencephalography (EEG) has become a popular imaging method for BCI development (Stangl, Bauernfeind, Kurzmann, Scherer, & Neuper, 2013). Though popular, an EEG-based

BCI is limited by poor spatial resolution, high sensitivity to noise and motion, and would be impractical for daily use due to its complicated setup process (Coyle, Ward, & Markham, 2007).

While EEG directly measures the electrical activity of the brain, functional near-infrared spectroscopy (fNIRS) measures brain activity indirectly through changes in blood oxygen content in the brain (León-Carrión & León-Domínguez, 2012). Though fNIRS lacks the temporal resolution of EEG, it benefits from higher spatial resolution, relatively low sensitivity to noise and movement, and a simple setup procedure (Stangl et al., 2013; León-Carrión & León-Domínguez, 2012; Hu, Hong, & Ge, 2011).

Previous research has evaluated the performance of fNIRS in BCI applications with varying degrees of success. In 2009, Matsuyama, Asama, and Otake designed a system which classified brain activity arising from mental arithmetic exercises into control signals for a humanoid robot. While their system was effective in controlling the robot, they found that faster response times would be necessary for any practical applications (Matsuyama et al., 2009). Waldert, Tushaus, Kaller, Aertsen, and Mehring (2012) attempted to design a BCI system which relied on hand movements rather than mental arithmetic. They concluded that fNIRS is not viable for decoding movement direction. Despite their conclusions, it is possible that the low classification accuracy they obtained was due to an optode layout that failed to target motor areas of the brain and a motor task which may have been unnatural for participants to perform.

Other researchers have been more successful with their attempts to develop NIRS-based BCI systems. For example, Naseer and Hong (2013) observed hemodynamic responses during 10 second trials in which participants were instructed to imagine repeatedly flexing either the right or left wrist. Classification accuracy using linear discriminate analysis was 73.35% for the right wrist and 83.00% for the left wrist (Naseer & Hong, 2013). In 2015, the same researchers

performed a similar experiment in which participants performed one of four tasks: mental arithmetic, mental counting, left-hand motor imagery, and right-hand motor imagery. Hemodynamic responses during these tasks were classified using linear discriminant analysis with an average accuracy of 73.30% (Naseer & Hong, 2015).

While these experiments demonstrate the potential for fNIRS to be used successfully in a BCI, neither of them offers a true solution for classifying motor activity in the brain in a way that mirrors the intended motor control of external peripherals. Each experiment described sought to generate control signals through specific, often non-intuitive tasks. While mental counting and arithmetic might be easily co-opted control signals, they are less than ideal when it comes to real-world applications. Optimally, a BCI would derive control signals from tasks which closely represent the intended output of the BCI.

The present study evaluated the capabilities and limitations of fNIRS to assess its potential to be used in a BCI. Brain signals were measured during four different joystick movement directions, both real and imagined. We predicted that greater activation would be observed in channels over the sensorimotor cortex and supplementary motor area during motor execution, while motor imagery would lead to greater activity in channels over the premotor cortex and posterior parietal cortex (Xu et al., 2014; Sauvage, Jissendi, Seignan, Manto, & Habas, 2013; Hanakawa et al., 2003; Hermes et al., 2011; Holper, Scholkmann, Shalóm, & Wolf, 2012; Beinsteiner, Höllinger, Lindinger, Lang, & Berthoz, 1995; Aflalo et al., 2015; Connolly, Anderson, & Goodale, 2003; Zapparoli et al., 2013). Previous studies have also demonstrated reduced activation for motor imagery and greater lateralization for motor execution (Kraeutner, Gionfriddo, Bardouille, & Boe, 2014; Ueno et al., 2010). The posterior parietal cortex is associated with motor intention and was expected to play a critical role in the decoding of

movement direction (Connolly et al., 2003; Barany, Della-Maggiore, Viswanathan, Cieslak, & Grafton, 2014). By controlling for differences in movement rate, expanding cortical coverage to motor regions, and creating a paradigm in which the imagery task is strongly associated with the motor goal, this experiment was designed to enhance our understanding of the capabilities of fNIRS.

METHODS

PARTICIPANTS AND BEHAVIORAL MEASURES

Thirty-nine right-handed undergraduate students were recruited to participate in this study from the introductory psychology subject pool at Colorado State University. Students received course credit for their participation in the study. Left-hand dominant participants were identified using the Edinburgh Handedness Inventory (Oldfield, 1971) and excluded from the study. Additionally, a brief survey was administered to screen for any history of psychiatric diagnosis, neurological disorders, traumatic brain injury, and drug use. These exclusionary criteria were intended to minimize any variation in neural activity not due to the experimental task. Approval for the study was obtained from the Colorado State University Institutional Review Board and all students provided informed consent prior to their participation.

EXPERIMENTAL PARADIGM

Participants were seated at a desk facing an LCD computer monitor positioned at a distance of approximately 45 centimeters. To provide a measure of inhibition control and executive function, participants completed a brief go/no-go task (Criaud & Boulinguez, 2013; Simmonds, Pekar, & Mostofsky, 2008) before beginning the primary experimental paradigm. After completing the go/no-go task, participants were asked to rest their right arm on the desk while gripping a Logitech Extreme 3D Pro joystick for the duration of the experiment. EAR 3a foam insert earphones were inserted into each ear canal for presentation of an auditory pacing tone.

Each block began with a two-second text prompt of either, “Imagine,” or, “Execute,” followed by an arrow presented for 16 seconds pointing either up, down, left, or right (subtending approximately 18° of horizontal visual angle and 10° of vertical visual angle). Given that brain activity detected through near-infrared spectroscopy is greatly impacted by the participant’s rate of response (De Guio, Jacobson, Molteno, Jacobson, & Meintjes, 2012; Jochumsen, Niazi, Mrachacz-Kersting, Farina, & Dremstrup, 2013), an auditory pacing tone was presented at a rate of 1 Hertz throughout the duration of the experiment (SPL = 73.6 dB). The tone was created by modifying a 516 Hz tone using Audacity to make the tone more comfortable to listen to (Figure 1).

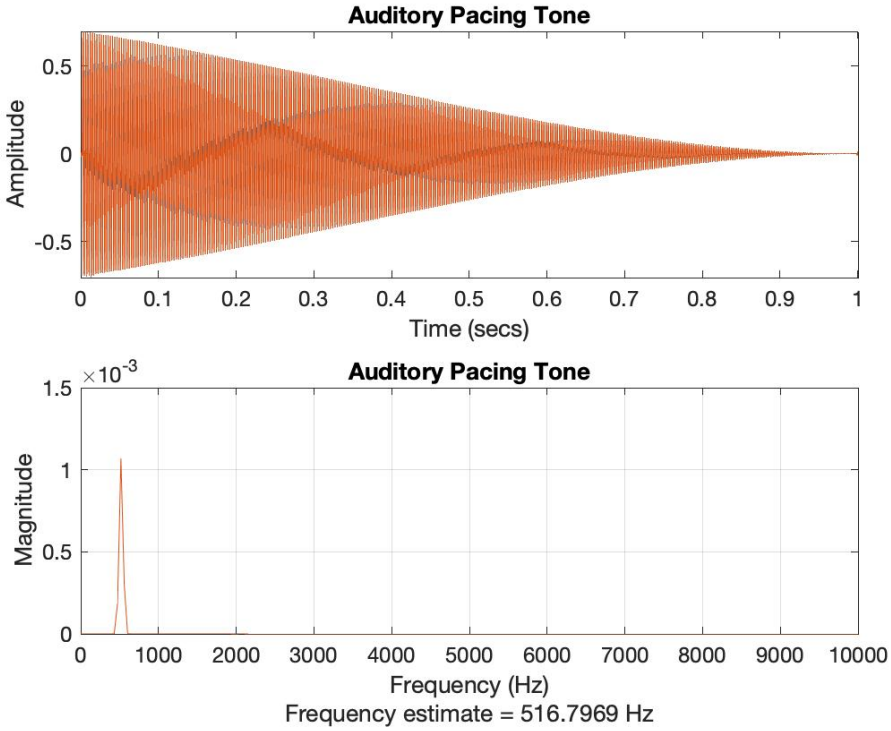

Figure 1. Time and frequency representation of the auditory pacing tone.

In the case of "Execute" trials, participants were asked to respond by repeatedly moving the joystick (allowing the joystick to return to center) in the direction indicated by the arrow in synchrony with the pacing tone. In the "Imagine" trials, participants were instructed to imagine moving the joystick at the same rate of repetition as the "Execute" trials but without initiating any overt movements.

Before starting the experiment, participants completed a short practice session during which their responses were monitored for both "Execute" and "Imagine" trials. This was done to ensure that participants understood the paradigm and engaged properly. Overall, the experimental design was a full factorial design with 2 levels of cue (“Execute” vs. “Imagine”) and 4 levels of direction (“Right”, “Left”, “Backward”, “Forward”), resulting in 8 unique block types. Each 18 second block was presented 7 times in pseudorandom order to each subject, along with 7, 18-second rest periods, for a total of 63 blocks (Figure 2). E-Prime 2 Professional was used to present the cues, as well as monitor joystick output. The total length of the experiment was 18 minutes and 54 seconds.

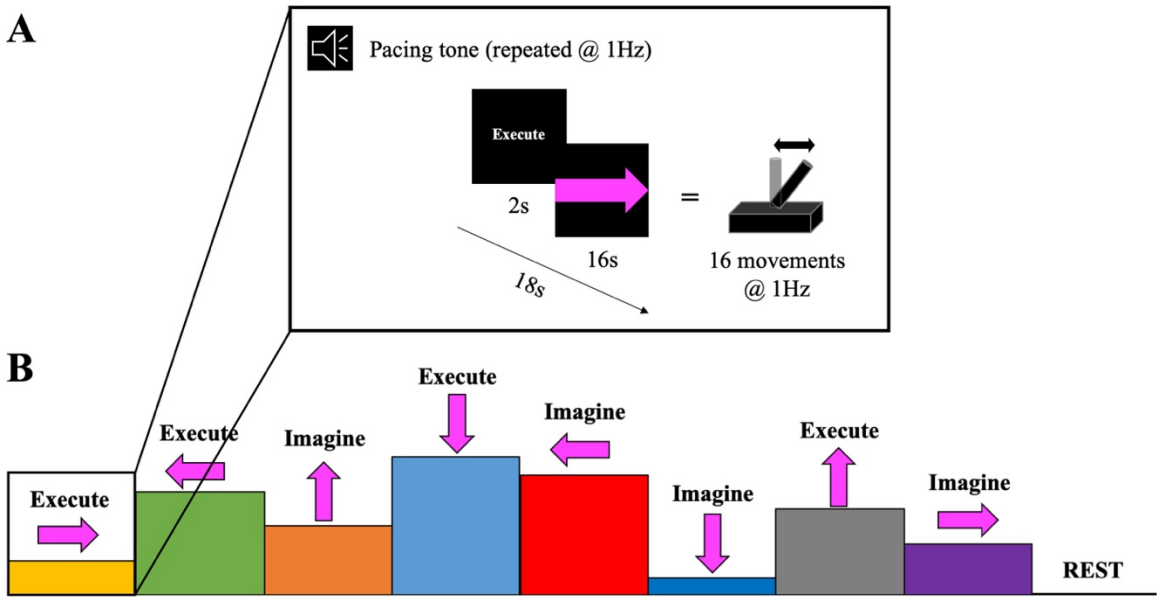

Figure 2. Visual representation of a single trial (A) and a single block (B). Each trial lasted 18 seconds and each block lasted 162 seconds. The experiment contained seven blocks for a total length of 18 minutes and 54 seconds.

NEAR-INFRARED SPECTROSCOPY DATA ACQUISITION

Hemodynamic changes associated with cortical activation were measured using continuous wave near-infrared spectroscopy. The NIRScoutX (NIRScout; NIRx Medical Technologies, Los Angeles, CA, USA) is capable of acquiring data from up to 32 silicon dioxide photodetectors simultaneously. 46 light-emitting diodes (LEDs) were utilized, emitting wavelengths of 760 and 850 nanometers at a sampling rate of 3.67 Hz. 134 channels were formed between sources and detectors within an optimal separation of 25-55mm (León-Carrión & León-Domínguez, 2012). This high-density array was designed to offer high spatial resolution while covering a large amount of cortical surface (Scholkmann, Spichtig, Muehlemann, & Wolf, 2010; Figure 3).

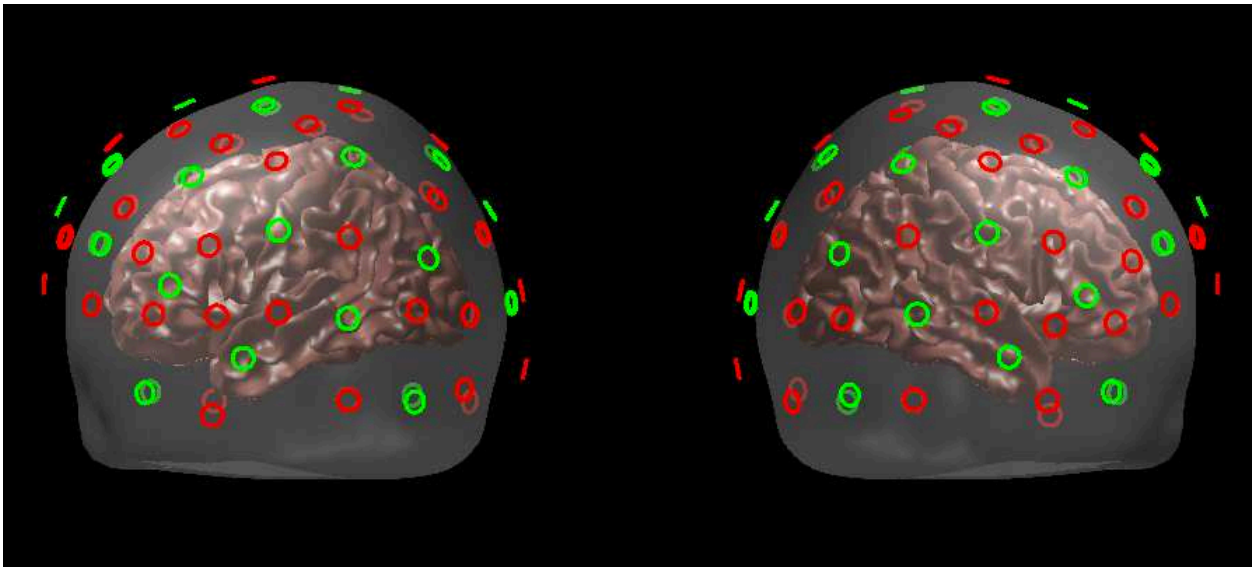

Figure 3: Visual representation of the approximate locations of sources (red circles) and detectors (green circles).

Optodes were manually inserted into NIRx spring-loaded grommets (NIRx Medical Technologies, Los Angeles, CA, USA)) embedded in EasyCap (cap montage M15) specialized recording caps (Easycap GmbH, Germany) in a standard 10-05 International Electrode system (Oostenveld & Praamstra, 2001). This ensured a relatively even and consistent distribution of optodes at an approximate spacing of three centimeters between optodes (Figure 4). The average channel distance calculated using 10-05 positions was 37.30 mm. Velcro chinstraps were used to secure caps and minimize cap movement.

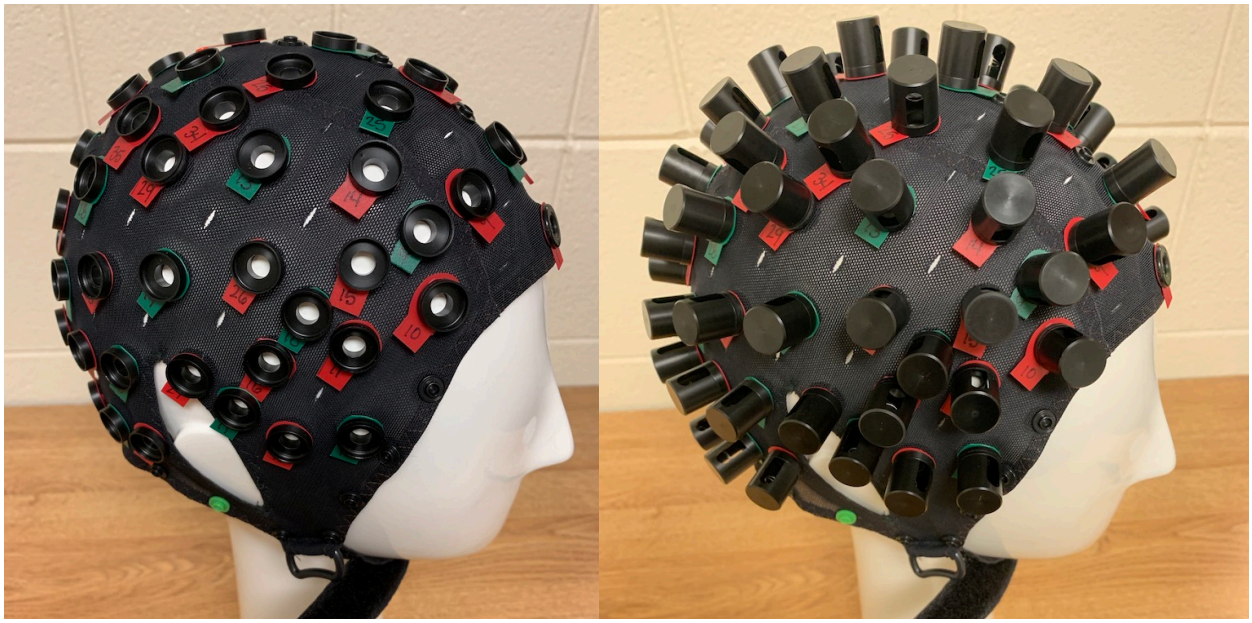

Figure 4. EasyCap (cap montage M15) specialized recording cap (Easycap GmbH, Germany) with (right) and without (left) NIRx spring-loaded grommets (NIRx Medical Technologies, Los Angeles, CA, USA)) embedded in a standard 10-05 International Electrode system (Oostenveld & Praamstra, 2001).

JOYSTICK DATA ACQUISITION

Joystick data was measured during both motor execution trials and motor imagery trials. The direction and amplitude of joystick deviation was acquired through a serial port with a BAUD rate of 9,600 Hz. Joystick response data were used to evaluate response accuracy during executed movement conditions. Additionally, erroneous responses during imagined movement conditions were identified by the presence of joystick deviations when no movement should occur.

ACCELEROMETER DATA ACQUISITION

To better identify erroneous responses during imagined movement conditions, a 3-axis accelerometer (g.Tec GmbH) was attached to the right forearm of the participant. The 3 channels of motion were digitized at 256 Hz and 24-bit resolution by a g.Tec HIamp amplifier system. While the accelerometer data could not be used to accurately identify movement

directions during executed movement conditions, because there was no calibration done after placement on the arm, it offered a highly sensitive secondary measure to detect minor muscle movements which may have occurred during imagined movement conditions. It is possible that these minor movements could impair our ability to accurately detect and classify imagined movements across subjects.

NEAR-INFRARED SPECTROSCOPY DATA ANALYSIS

fNIRS channel positions were transformed into their positions in the Montreal Neurological Institute (MNI) brain space. Next, the measured changes in light absorption were converted to changes in oxygenated hemoglobin concentrations utilizing the modified Beer-Lambert law (Delpy et al., 1988; Khan et al., 2014; Huppert, Diamond, Franceschini, & Boas, 2009). The "movement artifact reduction algorithm" (Scholkmann et al., 2010) was utilized to correct for any motion artifacts present in the data. This technique was implemented in MATLAB using the SPM-fNIRS toolbox (Brigadoi et al., 2013; Scholkmann et al., 2010). After removing motion artifacts, band-pass filtering was used to remove frequencies above 0.20 Hz and below 0.01 Hz. This was done to remove high-frequency instrumental noise and to reduce low-frequency biological noise associated with cardiac artifacts, respiratory signals, and blood pressure changes known as the Mayor wave (Huppert et al., 2009). The initial sampling rate of 3.68 Hz was resampled to 0.99 Hz. This was done to improve compatibility with SPM and was necessary for motion artifact rejection analysis.

Oxygenated hemoglobin (HbO) data were subjected to first level analysis using a general linear model (GLM) approach implemented in spm_fnirs (Tak, Uga, Flandin, Dan, & Penny, 2016) incorporating a regressor formed by applying an HRF-convolved boxcar function to the block design. Second level analyses were performed using one-sample t tests to identify

channels with significant differences in measured activation. Multiple comparisons were corrected for using a False Discovery Rate (FDR) approach.

Three contrasts were formed to compare activation of all executed movements relative to baseline, all imagined movements relative to baseline, and all executed movements compared to imagined movements. Eight more contrasts were used to compare each individual executed movement direction to the other three executed movement directions and each imagined movement direction to the other three imagined movement directions.

JOYSTICK DATA ANALYSIS

Joystick data was baseline corrected and filtered using a 20 Hz low-pass phase-invariant 2nd order Butterworth filter. Next, the number and amplitude of each detected movement in each block was obtained for each trial using the findpeaks.m function from Matlab (Figure 5). Overall movement accuracy was calculated and displayed for each block, along with movement amplitude. Joystick data was then downsampled from 9,600 Hz to match the resampled NIRS sampling rate of 0.99 Hz. This was necessary for performing NIRS analyses using joystick data as a regressor.

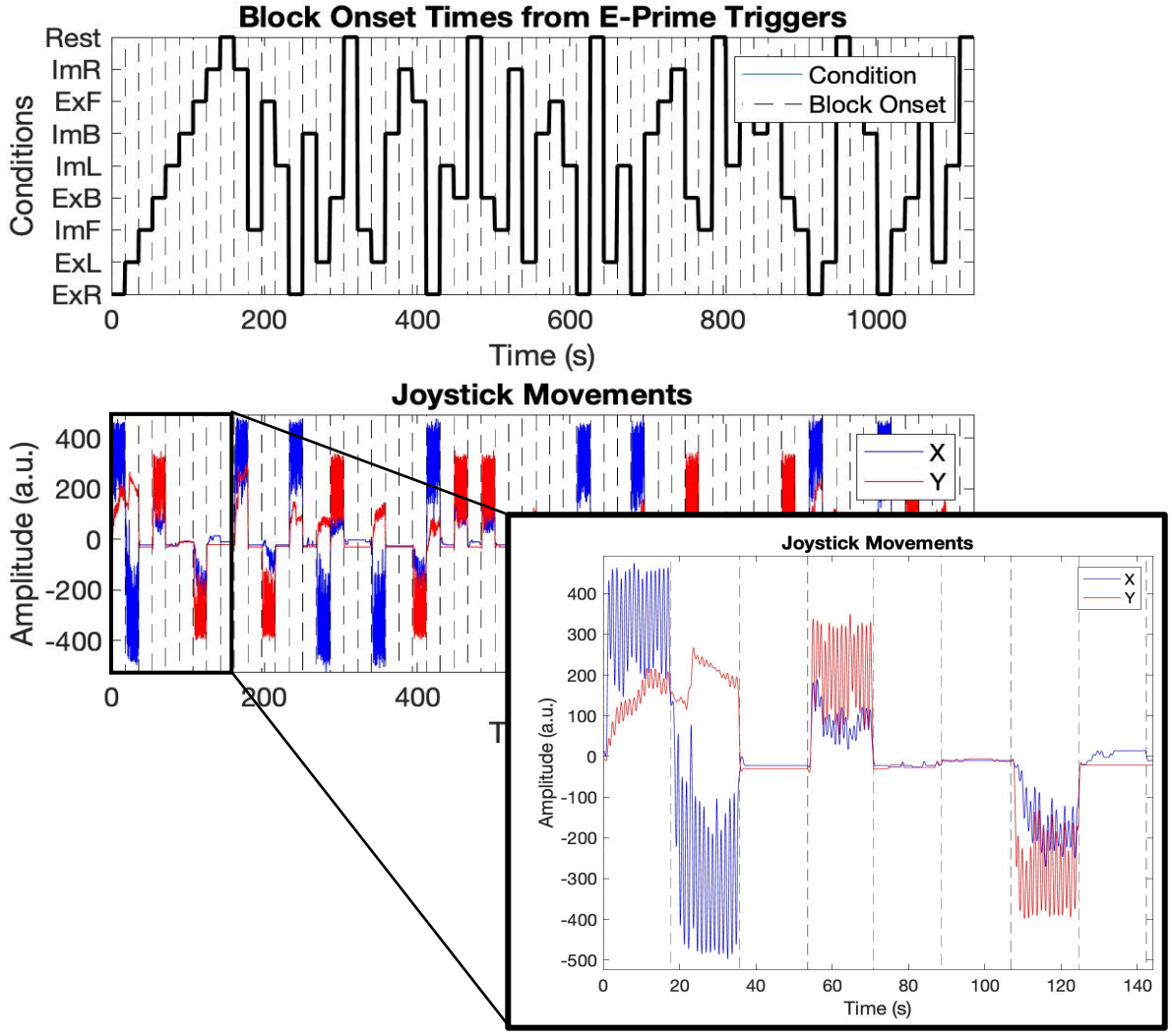

Figure 5. Example output of joystick movements and block design. Right and left movements are indicated by postive and negative x values, respectively. Forward and back movevements are indicated by negative and positive y values, respectively. The enlarged section shows activity during the first 8 blocks.

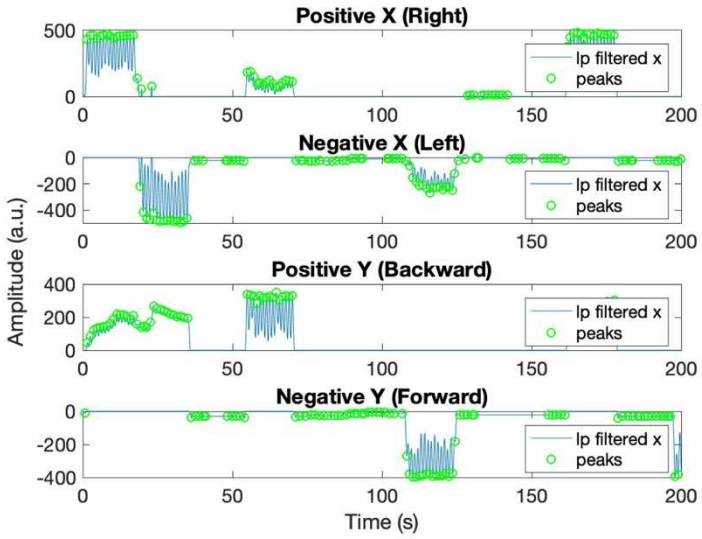

Figure 6. Single subject joystick data organized by movement direction. Green circles indicate peaks identified. For accuracy calculations, only peaks occurring during the correct movement direction counted towards accuracy score.

ACCELEROMETER DATA ANALYSIS

Accelerometer data was analyzed using custom scripts implemented in MATLAB. First, the accelerometer scale was converted and the DC offset was removed. Band-pass filtering was applied using two-way least square finite impulse response filters with an order of 3072, beginning with a high-pass filter of 10 Hz followed by a low-pass filter of 0.25 Hz. Data were then epoched into 1024 sample epochs and downsampled to match the resampled NIRS sampling rate of 0.99 Hz. Finally, a root mean square transformation was performed to convert x, y, and z values to a single movement amplitude.

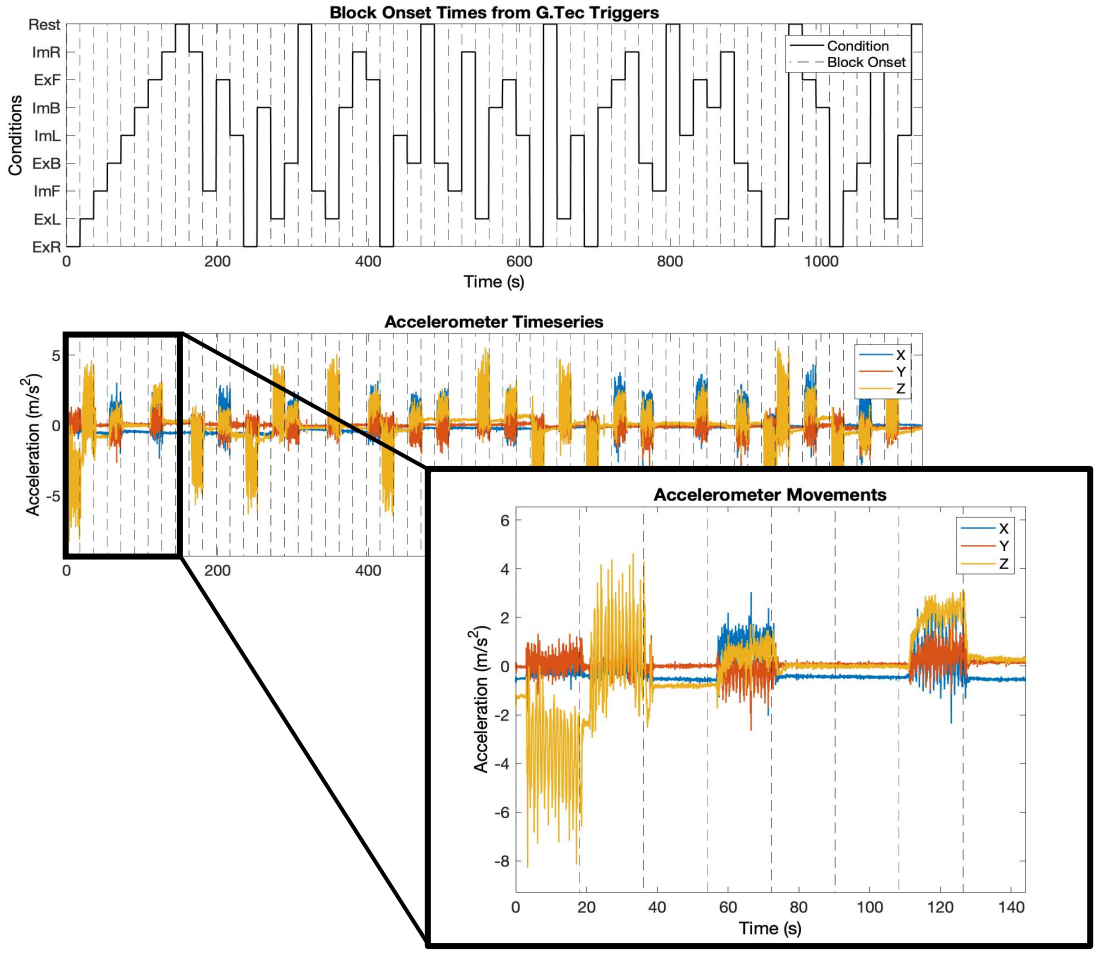

Figure 7. Example output of accelometer data and block design. Given that there was no calibration done after placement on the arm, x, y, and z values have no utility apart from serving as a highly sensitive secondary measure to detect minor muscle movements which may have occurred during imagined movement conditions. The enlarged section shows activity during the first 8 blocks.

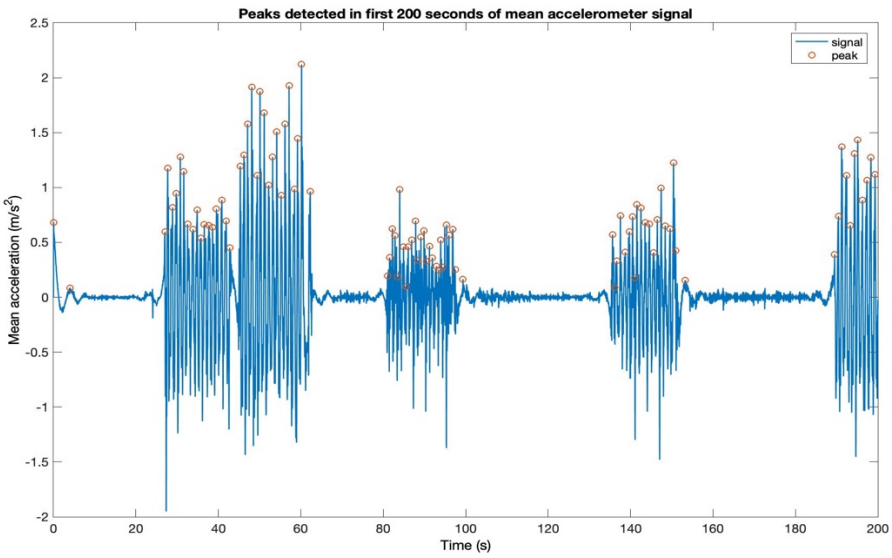

Figure 8. Single subject mean accelerometer data during the first 200 seconds of the experiment. Peaks are indicated by orange circles.

RESULTS

FNIRS RESULTS

Eleven participants were eliminated from analysis due to inadequate quality of measured spectroscopy data. 28 participants were included in the analyses. For each channel formed in the optode array, the effect of movement condition and direction on oxygenated hemoglobin levels was assessed using one-sample t-tests with a False Detection Rate (FDR) correction for multiple comparisons. No significant differences in inferred cortical activation were observed between individual movement directions. When comparing executed movements to baseline activity, 20 channels measured significant changes in oxygenated hemoglobin levels (Figure 9). When comparing imagined movements to baseline, significant changes in oxy-Hb levels were measured in 21 channels (Figure 10). When comparing executed movements to imagined movements, four channels measured significant changes in oxy-Hb levels (Figure 11; Table 1).

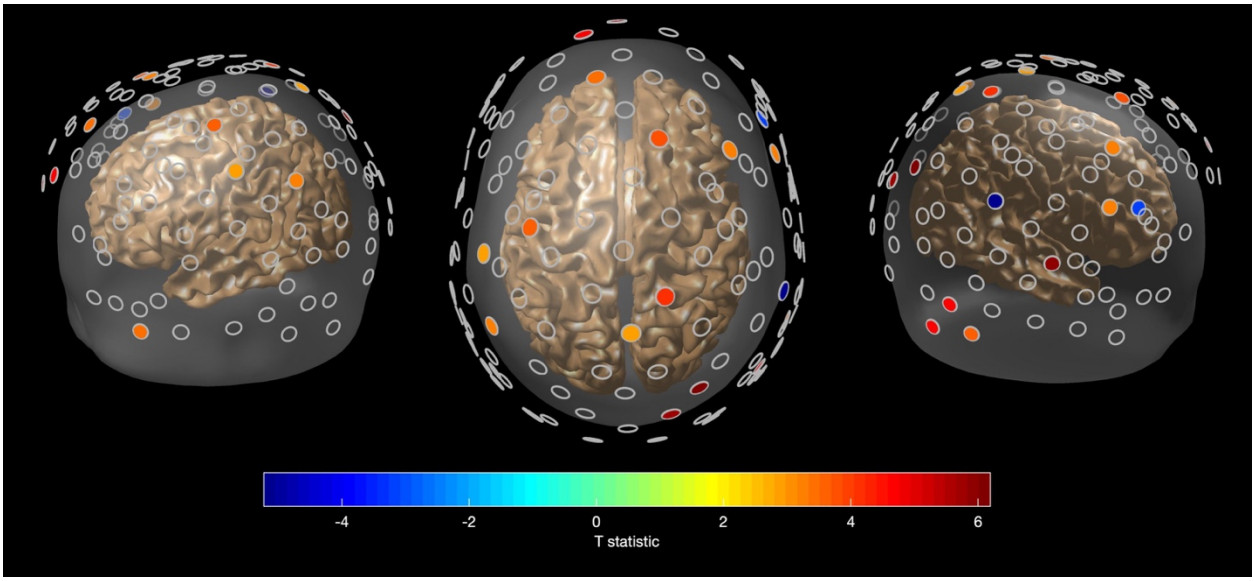

Figure 9. Channels reflecting significant changes in hemodynamic activity during executed movement conditions compared to baseline. Red activation patterns correspond to greater oxy-Hb levels while blue regions correspond to reduced oxy-Hb levels.

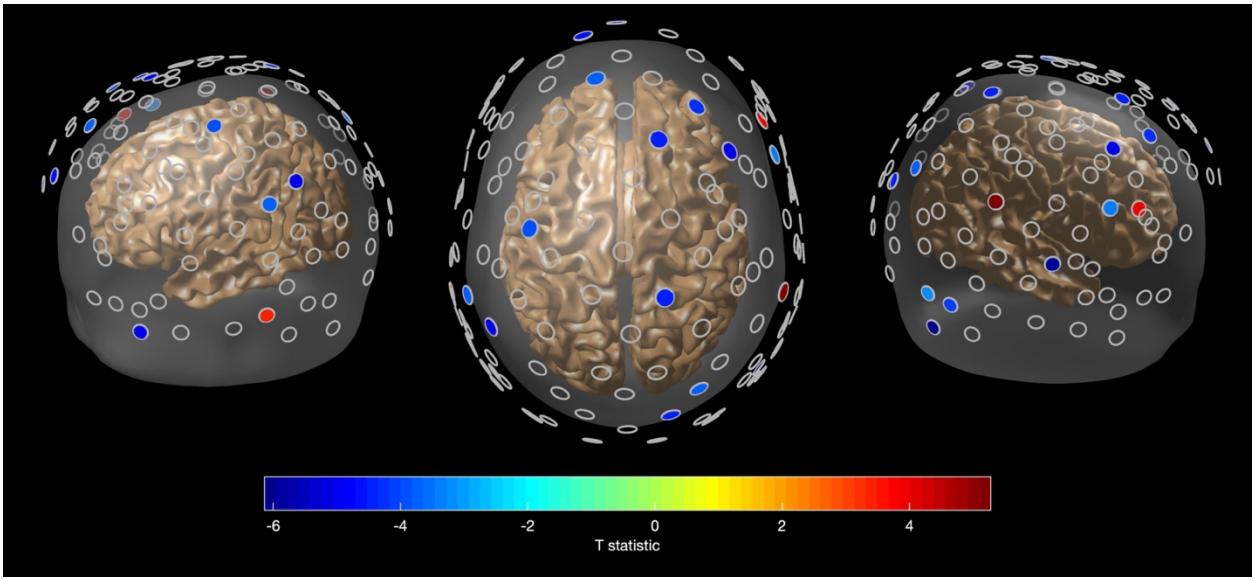

Figure 10. Channels reflecting significant changes in hemodynamic activity during imagined movement conditions compared to baseline. Red activation patterns correspond to greater oxy-Hb levels while blue regions correspond to reduced oxy-Hb levels.

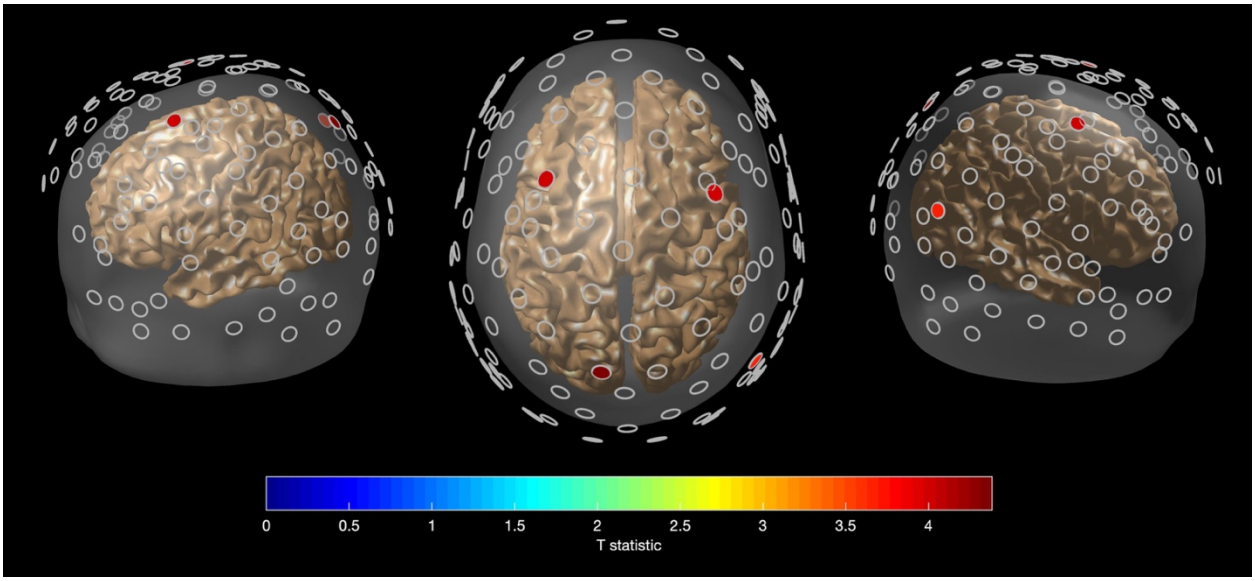

Figure 11. Channels reflecting significant changes in hemodynamic activity during executed movement conditions compared to imagined movement conditions. Red activation patterns correspond to greater oxy-Hb levels while blue regions correspond to reduced oxy-Hb levels.

Table 1. *Channels with significant changes in HbO levels. MNI coordinates are listed for the channels, and 10-05 labels are given for source-detector pairs. AAL2 brain areas were determined using the fOLD application for Matlab 2017a.*

Brain Area	NIRS Channel	S-D Pair	Channel Location			*t* value	*p*
			X	Y	Z		
Execute>Baseline							
Frontal Lobe (Medial)	1	Fpz - AFz	2.33	66.00	-19.67	5.40	.0000
Frontal Lobe (Left)	2	AF3 - AFz	-12.67	69.00	-14.67	4.62	.0001
Temporal Lobe (Left)	16	FT9 - F9	-47.33	5.67	-45.67	3.48	.0017
Frontal Lobe (Left)	29	Fz - F1	-11.33	66.33	27.00	3.36	.0023
Frontal Lobe (Right)	35	F6 - FC4	58.00	30.67	-1.67	-3.14	.0041
Parietal Lobe (Left)	52	C3 - CP3	-67.00	-32.67	37.33	2.95	.0064
Frontal Lobe (Right)	62	FC2 - FC4	55.33	23.33	35.00	3.33	.0025
Supplementary Motor Area (Right)	64	FC2 - FCz	18.00	31.67	60.67	3.72	.0009
Precentral Gyrus (Right)	67	FC6 - FC4	61.33	15.33	5.67	3.19	.0036
Temporal Lobe (Right)	70	T8 - C6	72.00	-20.33	-15.33	5.85	.0000
Cerebellum (Right)	74	TP10 - P10	52.67	-62.33	-46.67	3.57	.0013
Parietal Lobe (Right)	81	CP6 - CP4	67.00	-50.33	23.67	-5.23	.0000
Temporal Lobe (Right)	84	P8 - P10	52.67	-72.33	-33.67	4.60	.0001
Cerebellum (Right)	86	PO10 - P10	44.33	-78.67	-41.33	4.68	.0001
Parietal Lobe (Right)	96	CP2 - CPz	16.00	-51.67	77.00	4.10	.0003
Precuneus (Right)	100	Pz - CPz	-0.33	-64.67	63.00	2.93	.0068
Occipital Lobe (Right)	107	PO4 - P2	28.33	-89.33	36.33	6.19	.0000
Occipital Lobe (Right)	108	PO4 - POz	15.33	-99.33	25.67	5.75	.0000
Postcentral Gyrus (Left)	116	CCP3h - C1	-48.67	-19.33	62.67	3.68	.0010
Parietal Lobe (Left)	122	P3 - CP3	-55.67	-67.00	37.33	3.33	.0025
Imagine>Baseline							
Frontal Lobe (Medial)	1	Fpz - AFz	2.33	66.00	-19.67	-5.17	.0000
Frontal Lobe (Left)	2	AF3 - AFz	-12.67	69.00	-14.67	-4.56	.0001
Temporal Lobe (Left)	16	FT9 - F9	-47.33	5.67	-45.67	-4.95	.0000
Frontal Lobe (Left)	29	Fz - F1	-11.33	66.33	27.00	-3.79	.0008
Frontal Lobe (Right)	35	F6 - FC4	58.00	30.67	-1.67	3.89	.0006
Temporal Lobe (Left)	47	TP9 - TP7	-55.00	-53.67	-38.33	3.43	.0019
Parietal Lobe (Right)	54	CP5 - CP3	-66.33	-51.00	23.33	-3.65	.0011
Frontal Lobe (Right)	62	FC2 - FC4	55.33	23.33	35.00	-4.91	.0000
Frontal Lobe (Right)	63	FC2 - F2	37.33	46.33	37.33	-4.22	.0002
Supplementary Motor Area (Right)	64	FC2 - FCz	18.00	31.67	60.67	-4.44	.0001
Precentral Gyrus (Right)	67	FC6 - FC4	61.33	15.33	5.67	-3.36	.0023
Temporal Lobe (Right)	70	T8 - C6	72.00	-20.33	-15.33	-5.94	.0000
Parietal Lobe (Right)	81	CP6 - CP4	67.00	-50.33	23.67	5.28	.0000
Temporal Lobe (Right)	84	P8 - P10	52.67	-72.33	-33.67	-4.01	.0004
Cerebellum (Right)	86	PO10 - P10	44.33	-78.67	-41.33	-6.14	.0000
Parietal Lobe (Right)	96	CP2 - CPz	16.00	-51.67	77.00	-4.43	.0001
Occipital Lobe (Right)	107	PO4 - P2	28.33	-89.33	36.33	-3.76	.0008
Occipital Lobe (Right)	108	PO4 - POz	15.33	-99.33	25.67	-4.53	.0001
Occipital Lobe (Right)	111	PO8 - P10	46.00	-81.00	-28.00	-3.19	.0035
Postcentral Gyrus (Left)	116	CCP3h - C1	-48.67	-19.33	62.67	-3.97	.0005
Parietal Lobe (Left)	122	P3 - CP3	-55.67	-67.00	37.33	-4.91	.0000
Execute>Imagine							
Frontal Lobe (Left)	41	FC1 - C1	-40.67	8.00	61.00	4.03	.0004
Frontal Lobe (Right)	93	FCC4h - C2	50.33	0.00	56.33	4.03	.0004
Precuneus (Left)	101	Pz - P1	-13.33	-81.00	55.67	4.38	.0002
Angular Gyrus (Right)	106	P4 - P6	51.67	-78.33	22.33	3.67	.0011

In addition to the above whole brain analysis, several other analyses were performed. First, data were analyzed based on regions of interest. These included the motor cortex, supplementary motor area, and posterior parietal cortex. Channels were grouped by region using the fOLD toolbox in Matlab (Morais, Balardin, & Sato, 2018). For this analysis, no significant differences were observed in any of the contrasts. To account for task accuracy, data were also analyzed using joystick accuracy and accelerometer measurements as predictors. No significant results were observed.

BEHAVIORAL RESULTS

Group-level performance measures for the Go/No-Go task indicated that participants performed accurately (M = 95.16%, SD = 5.44%). On average, subjects made 2.32 ± 2.61 errors during the Go/No-Go task with an average error of commission rate of 1.29 ± 1.30.

An ANOVA was performed on processed joystick data and indicated no significant differences in accuracy between executed movement directions ($F(3, 108) = 0.75$, $p = .52$). A second ANOVA was used to assess whether or not there was a difference in movement amplitude during correctly executed joystick movement conditions. Results indicated there was a significant difference in movement amplitude ($F(3, 108) = 70.58$, $p < .001$). Tukey HSD post-hoc tests indicated that subjects moved the joystick more during right (M = 409.49, SD = 41.84) and left (M = 427.14, SD = 48.11) movement conditions compared to forward (M = 347.84, SD = 39.34) and back (M = 286.48, SD = 29.62) conditions. Additionally, participants moved the joystick more during forward movements (M = 347.84, SD = 39.34) compared to back movements (M = 286.48, SD = 29.62; Figure 12).

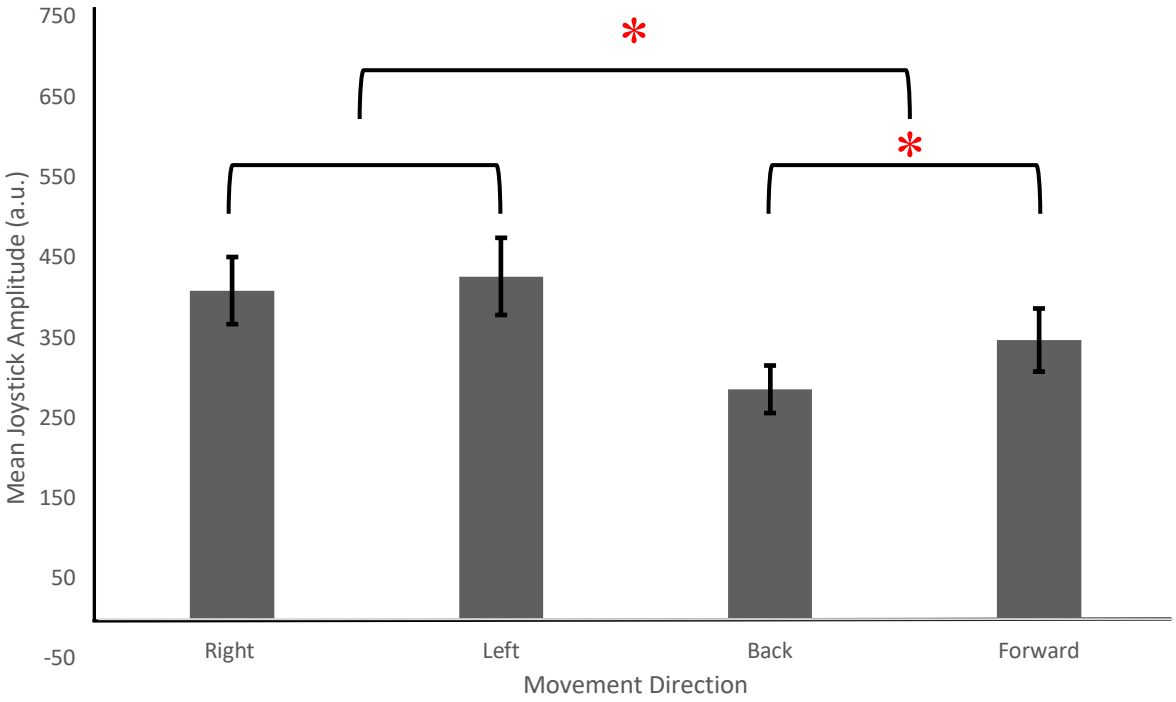

Figure 12. Bar graph indicating mean joystick amplitudes for each of the four movement directions. Participants moved the joystick with greater amplitude during right and left conditions compared to forward and back conditions. Participants also moved the joystick more during forward conditions compared to back conditions.

DISCUSSION

The results of the preprocessing and analysis methods used in this study indicated significant differences in inferred cortical activation during both executed and imagined movements compared to baseline. There were also significant differences between executed and imagined movement conditions. For individual movement directions, no significant differences were observed for executed or imagined conditions.

Relative to baseline, inferred cortical activation during all executed movement conditions was greater in the right pre-motor cortex, right pre-supplementary motor area, left motor cortex, right motor or somatosensory cortex, and the posterior parietal cortex. During the imagined movement conditions, inferred cortical activation was reduced relative to baseline in the right pre-supplementary motor area, right pre-motor cortex, left motor cortex, and the right somatosensory cortex. When comparing the executed movement conditions to imagined movement conditions, the left and right pre-motor or motor cortices displayed greater activation in the execute conditions. This finding did not conform with our expectation based on previous literature, which suggested the sensorimotor cortex and supplementary motor areas would show greater activation during motor execution while the premotor cortex and posterior parietal cortex would be more active during motor imagery (Xu et al., 2014; Sauvage, Jissendi, Seignan, Manto, & Habas, 2013; Hanakawa et al., 2003; Hermes et al., 2011; Holper, Scholkmann, Shalóm, & Wolf, 2012; Beinsteiner, Höllinger, Lindinger, Lang, & Berthoz, 1995; Aflalo et al., 2015; Connolly, Anderson, & Goodale, 2003; Zapparoli et al., 2013).

An initial interpretation of the outcomes of this study is that fNIRS is not capable of detecting differences in brain activity associated with small movements such as joystick

movement directions. This interpretation upholds the findings of numerous research studies (Waldert et al., 2012). However, it is possible that the traditional methods used for analyzing fNIRS data may have had a negative impact on our ability to detect and classify movement directions. In fMRI literature, research has shown that correction for motion may interfere with the detection of signals of interest during motion-based tasks (Seto et al., 2001). Given that movement is a primary component of this study, it is possible that eliminating motion artifacts also eliminates motion data corresponding to signals of interest.

Another factor which may have had a detrimental effect on results was the movement itself. During the executed movement conditions, participants always returned the joystick to the center position between each joystick movement. Therefore, when executing a right joystick movement, the actual motor activity was always composed of a right movement and a left movement back to center. While the return to center was assisted by the joystick, it is possible that this two-way movement hindered the ability to detect individual movement directions.

Behavioral results logged by the joystick also showed that right and left movements were often mixed with slight forward/backward deviations and vice versa. These impure movements may have added to the difficulty of classifying individual movement directions. Additionally, moving the joystick forward and backward requires a larger overall movement, given that the arm is typically lifted from the table somewhat to engage the movement. Left and right directions, on the other hand, require smaller movements given that only the wrist is moved. This effect can be observed in the results of the joystick amplitude analysis, which showed that participants moved the joystick a greater distance during right and left movement conditions compared to forward and back conditions, where movement may have been more difficult.

The purpose of the present study was to evaluate the capabilities and limitations of fNIRS with an emphasis on BCI applications. By controlling for differences in movement rate, expanding cortical coverage to provide a whole-head analysis, and utilizing movements which closely mirror the intended motor goal, the results of this study provide insight into the topic with fewer confounds than previous literature. Though the findings of this study do not present an optimistic view of the future of fNIRS in BCI, there are more questions that need to be addressed before a definitive conclusion is drawn. In the future, it would be worthwhile to perform a thorough analysis of the impact that various motion artifact rejection methods have on signals of interest in motor studies. Additionally, more robust cortical activation patterns for individual movement directions could be attained by adjusting the motor task to elicit pure directional movements.

Another option is to consider a bimodal BCI using both EEG and fNIRS for signal acquisition. Because fNIRS uses light emission, it does not interfere with EEG and therefore, pairs very well with EEG for multimodal neuroimaging. To address some of the limitations of EEG-based BCIs, many researchers have attempted to develop bimodal BCIs using EEG and functional near-infrared spectroscopy (fNIRS) simultaneously. By pairing fNIRS with EEG, classification accuracy of BCI is generally improved. In a motor imagery task involving hand gripping with visual feedback, Fazli et al. (2012) observed an increased accuracy in over 90% of participants with a 5% improvement on average. While these hybrid approaches offer improved classification accuracy by taking advantage of the proficiencies of each modality, they also suffer from all of the aforementioned drawbacks with respect to real-world practicality. These limitations should be carefully considered when designing multimodal BCIs.

Regardless of the imaging method, a promising direction for the future of data analysis utilizes machine learning algorithms to process and analyze data. In order to implement a BCI, it would be necessary to analyze and classify joystick movements in real time, without experimenter intervention. Not only do machine learning algorithms achieve this, research also suggests that they may provide better classification accuracy than traditional data analysis methods, such as those used in this study (Sitaram et al., 2015; Matthews, Pearlmutter, Wards, Soraghan, & Markham, 2008). By adjusting the motor task and implementing a machine learning algorithm, future research could lead to an improved understanding of the capabilities and limitations of fNIRS.

REFERENCES

Aflalo, T., Kellis, S., Klaes, C., Lee, B., Shi, Y., Pejsa, K., ... & Liu, C. (2015). Decoding motor imagery from the posterior parietal cortex of a tetraplegic human. *Science*, *348*(6237), 906-910.

Barany, D. A., Della-Maggiore, V., Viswanathan, S., Cieslak, M., & Grafton, S. T. (2014). Feature interactions enable decoding of sensorimotor transformations for goal-directed movement. *The Journal of Neuroscience*, *34*(20), 6860-6873.

Beisteiner, R., Höllinger, P., Lindinger, G., Lang, W., & Berthoz, A. (1995). Mental representations of movements. Brain potentials associated with imagination of hand movements. *Electroencephalography and Clinical Neurophysiology/Evoked Potentials Section*, *96*(2), 183-193.

Brigadoi, S., Ceccherini, L., Cutini, S., Scarpa, F., Scatturin, P., Selb, J., ... & Cooper, R. J. (2014). Motion artifacts in functional near-infrared spectroscopy: a comparison of motion correction techniques applied to real cognitive data. *Neuroimage*, *85*, 181-191.

Carlson, T., & Millan, J. D. R. (2013). Brain-controlled wheelchairs: a robotic architecture. *IEEE Robotics and Automation Magazine*, *20*(EPFL-ARTICLE-181698), 65-73.

Collinger, J. L., Wodlinger, B., Downey, J. E., Wang, W., Tyler-Kabara, E. C., Weber, D. J., ... & Schwartz, A. B. (2013). High-performance neuroprosthetic control by an individual with tetraplegia. *The Lancet*, *381*(9866), 557-564.

Connolly, J. D., Andersen, R. A., & Goodale, M. A. (2003). FMRI evidence for a parietal reach region in the human brain. *Experimental Brain Research*,*153*(2), 140-145.

Coyle, S. M., Ward, T. E., & Markham, C. M. (2007). Brain–computer interface using a simplified functional near-infrared spectroscopy system. *Journal of Neural Engineering*, *4*(3), 219.

Criaud, M., & Boulinguez, P. (2013). Have we been asking the right questions when assessing response inhibition in go/no-go tasks with fMRI? A meta-analysis and critical review. *Neuroscience & biobehavioral reviews, 37*(1), 11-23.

De Guio, F., Jacobson, S. W., Molteno, C. D., Jacobson, J. L., & Meintjes, E. M. (2012). Functional magnetic resonance imaging study comparing rhythmic finger tapping in children and adults. *Pediatric Neurology*, *46*(2), 94-100.

Delpy, D. T., Cope, M., van der Zee, P., Arridge, S. R., Wray, S., & Wyatt, J. S. (1988). Estimation of optical pathlength through tissue from direct time of flight measurement. *Physics in Medicine and Biology*, *33*(12), 1433.

Desmond, J. E., & Glover, G. H. (2002). Estimating sample size in functional MRI (fMRI) neuroimaging studies: statistical power analyses. *Journal of Neuroscience Methods*, *118*(2), 115-128.

Fazli, S., Mehnert, J., Steinbrink, J., Curio, G., Villringer, A., Müller, K. R., & Blankertz, B. (2012). Enhanced performance by a hybrid NIRS–EEG brain computer interface. *Neuroimage*, *59*(1), 519-529.

Galán, F., Nuttin, M., Lew, E., Ferrez, P. W., Vanacker, G., Philips, J., & Millán, J. D. R. (2008). A brain-actuated wheelchair: asynchronous and non-invasive brain–computer interfaces for continuous control of robots. *Clinical Neurophysiology*, *119*(9), 2159-2169.

Hanakawa, T., Immisch, I., Toma, K., Dimyan, M. A., Van Gelderen, P., & Hallett, M. (2003). Functional properties of brain areas associated with motor execution and imagery. *Journal of Neurophysiology*, *89*(2), 989-1002.

Hermes, D., Vansteensel, M. J., Albers, A. M., Bleichner, M. G., Benedictus, M. R., Orellana, C. M., ... & Ramsey, N. F. (2011). Functional MRI-based identification of brain areas involved in motor imagery for implantable brain computer interfaces. *Journal of Neural Engineering*, *8*(2), 025007.

Holper, L., Scholkmann, F., Shalóm, D. E., & Wolf, M. (2012). Extension of mental preparation positively affects motor imagery as compared to motor execution: a functional near-infrared spectroscopy study. *Cortex*, *48*(5), 593-603.

Hu, X. S., Hong, K. S., & Ge, S. S. (2011). Recognition of stimulus-evoked neuronal optical response by identifying chaos levels of near-infrared spectroscopy time series. *Neuroscience Letters*, *504*(2), 115-120.

Hu, X. S., Hong, K. S., & Ge, S. S. (2013). Reduction of trial-to-trial variability in functional near-infrared spectroscopy signals by accounting for resting-state functional connectivity. *Journal of Biomedical Optics*, *18*(1), 017003-017003.

Huppert, T. J., Diamond, S. G., Franceschini, M. A., & Boas, D. A. (2009). HomER: a review of time-series analysis methods for near-infrared spectroscopy of the brain. *Applied Optics*, *48*(10), D280-D298.

Jochumsen, M., Niazi, I. K., Mrachacz-Kersting, N., Farina, D., & Dremstrup, K. (2013). Detection and classification of movement-related cortical potentials associated with task force and speed. *Journal of Neural Engineering*, *10*(5), 056015.

José León-Carrión and Umberto León-Domínguez (2012). Functional Near-Infrared Spectroscopy (fNIRS): Principles and Neuroscientific Applications, Neuroimaging - Methods, Prof. Peter Bright (Ed.), ISBN: 978-953- 51-0097-3, InTech, Available from: http://www.intechopen.com/books/neuroimaging-methods/functional-near- infrared-spectroscopy-fnirs-brain-studies-and-others-clinical-uses

Khan, M. J., Hong, K. S., Naseer, N., & Bhutta, M. R. (2014). A hybrid EEG-fNIRS BCI: Motor imagery for EEG and mental arithmetic for fNIRS. *Control, Automation and Systems (ICCAS), 2014 14th International Conference* (pp. 275-278). IEEE.

Khan, M. J., Hong, M. J., & Hong, K. S. (2014). Decoding of four movement directions using hybrid NIRS-EEG brain-computer interface. *Frontiers in Human Neuroscience*, *8*, 1-10.

Kraeutner, S., Gionfriddo, A., Bardouille, T., & Boe, S. (2014). Motor imagery-based brain activity parallels that of motor execution: Evidence from magnetic source imaging of cortical oscillations. *Brain research*, *1588*, 81-91.

Lorey, B., Naumann, T., Pilgramm, S., Petermann, C., Bischoff, M., Zentgraf, K., ... & Munzert, J. (2013). How equivalent are the action execution, imagery, and observation of intransitive movements? Revisiting the concept of somatotopy during action simulation. *Brain and Cognition*, *81*(1), 139-150.

Matsuyama, H., Asama, H., & Otake, M. (2009). Design of differential near-infrared spectroscopy based brain machine interface. *The 18th IEEE International Symposium on Robot and Human Interactive Communication* (pp. 775-780). IEEE.

Matthews, F., Pearlmutter, B. A., Wards, T. E., Soraghan, C., & Markham, C. (2008). Hemodynamics for brain-computer interfaces. *IEEE Signal Processing Magazine*, *25*(1), 87-94.

Morais, G. A. Z., Balardin, J. B., & Sato, J. R. (2018). fNIRS Optodes' Location Decider (fOLD): A toolbox for probe arrangement guided by brain regions-of-interest. *Scientific reports, 8*(1), 3341.

Munzert, J., Lorey, B., & Zentgraf, K. (2009). Cognitive motor processes: the role of motor imagery in the study of motor representations. *Brain Research Reviews*, *60*(2), 306-326.

Naseer, N., & Hong, K. S. (2013). Classification of functional near-infrared spectroscopy signals corresponding to the right-and left-wrist motor imagery for development of a brain–computer interface. *Neuroscience Letters*, *553*, 84-89.

Naseer, N., & Hong, K. S. (2015). Decoding answers to four-choice questions using functional near infrared spectroscopy. *Journal Near Infrared Spectroscopy*, *23*(1), 23-31.

Nicolas-Alonso, L. F., & Gomez-Gil, J. (2012). Brain computer interfaces, a review. *Sensors, 12*, 1211-1279.

Oldfield, R. C. (1971). The assessment and analysis of handedness: the Edinburgh inventory. *Neuropsychologia*, *9*(1), 97-113.

Oostenveld, R., & Praamstra, P. (2001). The five percent electrode system for high-resolution EEG and ERP measurements. *Clinical Neurophysiology*,*112*(4), 713-719.

Sauvage, C., Jissendi, P., Seignan, S., Manto, M., & Habas, C. (2013). Brain areas involved in the control of speed during a motor sequence of the foot: Real movement versus mental imagery. *Journal of Neuroradiology*, *40*(4), 267-280.

Scholkmann, F., Spichtig, S., Muehlemann, T., & Wolf, M. (2010). How to detect and reduce movement artifacts in near-infrared imaging using moving standard deviation and spline interpolation. *Physiological Measurement*, *31*(5), 649.

Seto, E., Sela, G., McIlroy, W. E., Black, S. E., Staines, W. R., Bronskill, M. J., ... & Graham, S. J. (2001). Quantifying head motion associated with motor tasks used in fMRI. *Neuroimage*, *14*(2), 284-297.

Simmonds, D. J., Pekar, J. J., & Mostofsky, S. H. (2008). Meta-analysis of Go/No-go tasks demonstrating that fMRI activation associated with response inhibition is task-dependent. *Neuropsychologia, 46*(1), 224-232.

Sitaram, R., Zhang, H., Guan, C., Thulasidas, M., Hoshi, Y., Ishikawa, A., ... & Birbaumer, N. (2007). Temporal classification of multichannel near-infrared spectroscopy signals of motor imagery for developing a brain–computer interface. *NeuroImage*, *34*(4), 1416-1427.

Stangl, M., Bauernfeind, G., Kurzmann, J., Scherer, R., & Neuper, C. (2013). A haemodynamic brain-computer interface based on real-time classification of near infrared spectroscopy signals during motor imagery and mental arithmetic. *Journal of Near Infrared Spectroscopy*, *21*(3), 157-171.

Tak, S., Uga, M., Flandin, G., Dan, I., & Penny, W.D. (2016). Sensor space group analysis for fNIRS data. *Journal of Neuroscience Methods*, 264, 103-112.

Ueno, T., Inoue, M., Matsuoka, T., Abe, T., Maeda, H., & Morita, K. (2010). Comparison between a real sequential finger and imagery movements: an fMRI study revisited. *Brain Imaging and Behavior*, *4*(1), 80-85.

Velliste, M., Perel, S., Spalding, M. C., Whitford, A. S., & Schwartz, A. B. (2008). Cortical control of a prosthetic arm for self-feeding. *Nature*,*453*(7198), 1098-1101.

Vučković, A., & Sepulveda, F. (2012). A two-stage four-class BCI based on imaginary movements of the left and the right wrist. *Medical Engineering & Physics*, *34*(7), 964-971.

Waldert, S., Tüshaus, L., Kaller, C. P., Aertsen, A., & Mehring, C. (2012). fNIRS exhibits weak tuning to hand movement direction. *PloS one*, *7*(11), e49266.

Wolpaw, J. R., & McFarland, D. J. (2004). Control of a two-dimensional movement signal by a noninvasive brain-computer interface in humans. *Proceedings of the National Academy of Sciences of the United States of America*, *101*(51), 17849-17854.

Xu, L., Zhang, H., Hui, M., Long, Z., Jin, Z., Liu, Y., & Yao, L. (2014). Motor execution and motor imagery: a comparison of functional connectivity patterns based on graph theory. *Neuroscience*, *261*, 184-194.

Ye, J. C., Tak, S., Jang, K. E., Jung, J., & Jang, J. (2009). NIRS-SPM: statistical parametric mapping for near-infrared spectroscopy. *Neuroimage*,*44*(2), 428-447.

Zapparoli, L., Invernizzi, P., Gandola, M., Verardi, M., Berlingeri, M., Sberna, M., ... & Paulesu, E. (2013). Mental images across the adult lifespan: a behavioural and fMRI investigation of motor execution and motor imagery. *Experimental Brain Research*, *224*(4), 519-540.

APPENDIX A

Go/No-Go Experimental Paradigm

Before participating in the primary experiment, participants completed a brief Go/No-Go experiment (Criaud & Boulinguez, 2013; Simmonds, Pekar, & Mostofsky, 2008). Forty-eight stimuli consisting of either "X" or "A" were presented randomly to the participant using E-Prime 2 Professional with an inter-stimulus interval of 700ms. When presented with an "X," participants were instructed to tap the spacebar as quickly as possible. When presented with an "A," participants were asked to refrain from responding. Go and No-Go trials appeared in equal proportions. Data were extracted from E-Prime and analyzed in Microsoft Excel.

APPENDIX B

Scripting Procedure for fNIRS Data Processing and Analysis

- Run script_convert_temporal_processing_Mathison.m
- Run nirx_condition_gui_batch_Don.m
- Run spatial processing in spm_fnirs to generate POS.mat file
- Run script_pos_correction.m
- Run script_spm_1st_level_stats_Mathison.m
- Run spm_fnirs_2ndlevel_onesamp_Mathison.m

APPENDIX C

Scripting Procedure for Joystick Data Processing and Analysis

- Run script_joystick_converter_Apr2018.m
- Run script_timing_correction_Apr2018.m on fNIRS data
- Copy “timings.txt” file into joystick data folder
- Run script_joystick_analyze_Feb2019.m

APPENDIX D

Scripting Procedure for Accelerometer Data Processing and Analysis

- Run script_timing_correction_Apr2018.m on fNIRS data
- Copy “timings.txt” file into accelerometer data folder
- Run script_analyze_gtec_accelerometer_Apr2019.m

APPENDIX E

Matlab Scripts

Matlab scripts for processing spectroscopy, accelerometer, and joystick data can be accessed at https://github.com/rojasdon/nirx_tools

APPENDIX F

R script to run ANOVA on joystick data

```
rm(list = ls())
library(nlme)
library(multcomp)
library(ggplot2)

#Find and read data
fname <- '/Users/Matt/Desktop/Joystick_stats.csv' #generate this from .txt file from analysis
script
data1 <- read.csv(fname)

## Accuracy ##
#Restructure data to prepare for ANOVA
r_acc <- data1[,c(1,74)]
r_acc[,3] <- colnames(r_acc[2])
names(r_acc)[c(2,3)] <- c("Accuracy","Movement_Direction")

l_acc <- data1[,c(1,75)]
l_acc[,3] <- colnames(l_acc[2])
names(l_acc)[c(2,3)] <- c("Accuracy","Movement_Direction")

b_acc <- data1[,c(1,76)]
b_acc[,3] <- colnames(b_acc[2])
names(b_acc)[c(2,3)] <- c("Accuracy","Movement_Direction")

f_acc <- data1[,c(1,77)]
f_acc[,3] <- colnames(f_acc[2])
names(f_acc)[c(2,3)] <- c("Accuracy","Movement_Direction")

acc_data <- rbind(r_acc, l_acc, b_acc, f_acc)
acc_data$id <- factor(acc_data$id)
acc_data$Movement_Direction <- factor(acc_data$Movement_Direction)


#Perform ANOVA
lme_anova_acc <- lme(Accuracy~Movement_Direction, data = acc_data, random = ~1|id)
summary(lme_anova_acc)

dir_anova_acc <- aov(Accuracy~Movement_Direction+Error(factor(id)/Movement_Direction),
data = acc_data)
summary(dir_anova_acc)
```

```
con_acc <- glht(lme_anova_acc,linfct=mcp(Movement_Direction="Tukey"))
summary(con_acc)

## Count ##
### MORE restructuring needed here ###

#Restructure data to prepare for ANOVA
r_count <- data1[,c(1,2)]
r_count[,3] <- colnames(r_count[2])
names(r_count)[c(2,3)] <- c("Count","Movement_Direction")

l_count <- data1[,c(1,3)]
l_count[,3] <- colnames(l_count[2])
names(l_count)[c(2,3)] <- c("Count","Movement_Direction")

b_count <- data1[,c(1,5)]
b_count[,3] <- colnames(b_count[2])
names(b_count)[c(2,3)] <- c("Count","Movement_Direction")

f_count <- data1[,c(1,4)]
f_count[,3] <- colnames(f_count[2])
names(f_count)[c(2,3)] <- c("Count","Movement_Direction")

count_data <- rbind(r_count, l_count, b_count, f_count)
count_data$id <- factor(count_data$id)
count_data$Movement_Direction <- factor(count_data$Movement_Direction)

#Perform ANOVA
lme_anova_count <- lme(Count~Movement_Direction, data = count_data, random = ~1|id)
summary(lme_anova_count)

dir_anova_count <- aov(Count~Movement_Direction+Error(factor(id)/Movement_Direction),
data = count_data)
summary(dir_anova_count)

con_count <- glht(lme_anova_count,linfct=mcp(Movement_Direction="Tukey"))
summary(con_count)

## Amplitude ##
#Restructure data to prepare for ANOVA
r_amp <- data1[,c(1,2)]
r_amp[,3] <- colnames(r_amp[2])
names(r_amp)[c(2,3)] <- c("Amplitude","Movement_Direction")

l_amp <- data1[,c(1,3)]
```

```
l_amp[,3] <- colnames(l_amp[2])
names(l_amp)[c(2,3)] <- c("Amplitude","Movement_Direction")

b_amp <- data1[,c(1,5)]
b_amp[,3] <- colnames(b_amp[2])
names(b_amp)[c(2,3)] <- c("Amplitude","Movement_Direction")

f_amp <- data1[,c(1,4)]
f_amp[,3] <- colnames(f_amp[2])
names(f_amp)[c(2,3)] <- c("Amplitude","Movement_Direction")

amp_data <- rbind(r_amp, l_amp, b_amp, f_amp)
amp_data$id <- factor(amp_data$id)
amp_data$Movement_Direction <- factor(amp_data$Movement_Direction)

#Perform ANOVA
lme_anova_amp <- lme(Amplitude~Movement_Direction, data = amp_data, random = ~1|id)
summary(lme_anova_amp)

dir_anova_amp <-
aov(Amplitude~Movement_Direction+Error(factor(id)/Movement_Direction), data = amp_data)
summary(dir_anova_amp)

con_amp <- glht(lme_anova_amp,linfct=mcp(Movement_Direction="Tukey"))
summary(con_amp)

#Plot Figure(s)
qplot(data=lme_anova_acc,
      x = variable,
      y = value,
      stat = "summary",
      fun.y = "mean",
      geom = c("point")
)
```